

Simon C. H. Yu
Wilbur C. K. Wong
Albert C. S. Chung
Kwok-Tung Lee
George K. C. Wong
Wai S. Poon

Does endoluminal coil embolization cause distension of intracranial aneurysms?

Received: 2 February 2006
Accepted: 18 April 2006
Published online: 29 June 2006
© Springer-Verlag 2006

S. C. H. Yu (✉) · K.-T. Lee
Department of Diagnostic Radiology
and Organ Imaging,
Prince of Wales Hospital,
30–32 Ngan Shing Street,
Shatin, NT Hong Kong,
People's Republic of China
e-mail: simonyu@cuhk.edu.hk
Tel.: +852-2632-2285
Fax: +852-2648-4122

W. C. K. Wong · A. C. S. Chung
Department of Computer Science,
Hong Kong University of Science
and Technology, Hong Kong,
People's Republic of China

G. K. C. Wong · W. S. Poon
Division of Neurosurgery,
Department of Surgery,
Prince of Wales Hospital,
Chinese University of Hong Kong,
Hong Kong, People's Republic
of China

Abstract *Introduction:* The aim of the present study was to determine whether intracranial aneurysms are distended after coil embolization and to evaluate the distensibility of ruptured aneurysms treated with endovascular coiling. *Methods:* This was a prospective study of 20 consecutive patients with 22 aneurysms, who presented with a ruptured cerebral aneurysm and were treated with endovascular coiling of the aneurysm in a single institution. A diagnostic digital subtraction angiography (DSA) and a three-dimensional radiographic angiography (3DRA) were performed with bi-plane angiography equipment (Philips V5000) immediately before and after the embolization procedure to detect volume enlargement of the aneurysm after embolization, and the extent of the enlargement. A simulation study with steel spheres was carried out to study the possible error of over-estimation of the postembolization volume due to the beam-hardening artifact. *Results:* There was no procedure-

related rupture of the aneurysms. The percentage by volume of solid coil within the coil mass ranged from 15.78% to 82.01% in the present series. All aneurysms showed distension which ranged from 0.09% to 34.23%. The distensibility of the aneurysms was 34.23%. Error due to the beam-hardening artifact was negligible. *Conclusion:* Endoluminal packing of intracranial saccular aneurysms with embolization coils could cause a certain degree of distension in aneurysms treated with coil embolization, with the degree of distension up to 34.2%. Intracranial aneurysms were able to tolerate a certain degree of endoluminal distension without a risk of immediate rupture, even those that had ruptured recently.

Keywords Intracranial aneurysms · Embolization · Endovascular procedures · Interventional neuroradiology · Three-dimensional radiographic angiography · Volumetric analysis

Introduction

A systematic review of studies involving 56,000 patients found that intracranial aneurysms occur in 3.6% to 6% of the general population [1]. Subarachnoid hemorrhage due to aneurysmal rupture is a dangerous event with a mortality rate as high as 50% [2]. Rupture of an intracranial aneurysm is known to occur in 6–8 per 100,000 in most Western population [3]. The 5-year cumulative rupture rate

of intracranial aneurysms for patients without a history of subarachnoid hemorrhage varies from 2.5% to 50% depending on the size and location of the aneurysm [4]. Annual rupture rates of 1.4% to 1.9% had been identified for intracranial aneurysms, with a higher rupture rate when aneurysms are larger than 10 mm in diameter, symptomatic, or located in the posterior circulation [1, 5]. Endovascular coiling has been accepted as an effective and safe nonsurgical alternative treatment for intracranial

aneurysms and has gained increasing popularity. It has been estimated that from 1995 to 2002, 100,000 patients with intracranial aneurysms have been treated with detachable coils [6]. Such treatment involves packing of coils into the lumen of the aneurysmal sac thereby occluding the aneurysm. The immediate protection against rupture occurs by reduction of blood pulsations within the fundus. An organized thrombus is formed within the aneurysm eventually, which is then covered by an endothelialized layer of connective tissue that covers the ostium of the neck [7, 8]. It is hypothesized that endoluminal packing of the aneurysmal sac could be associated with a certain degree of distension of the aneurysmal sac. The aim of the present study was to determine whether intracranial aneurysms are distended after coil embolization and to evaluate the distensibility of ruptured aneurysms treated with endovascular coiling.

Patients and methods

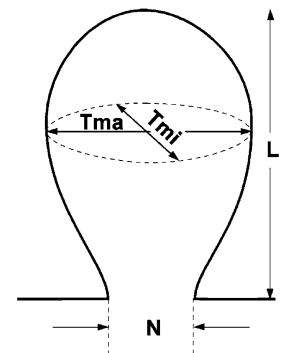
This was a prospective study which involved 20 consecutive patients who presented with subarachnoid hemorrhage due to a ruptured cerebral aneurysm and were treated with endovascular coiling of the aneurysm in a single institution. There were two aneurysms in two patients, making a total of 22 aneurysms. Subarachnoid hemorrhage was confirmed and the cerebral aneurysm detected with CT scan and CT angiography performed with a 16-detector CT scanner (General Electric) on admission to the institution. The CT images were examined by a neurosurgeon together with an interventional neuroradiologist who jointly made a decision to treat the patient with endovascular coiling. Specifically, evidence was sought of intraluminal thrombus within the aneurysm. Informed consent for endovascular coiling was obtained from each patient or a close relative when the patient was unable to give consent. Under general anesthesia, diagnostic digital subtraction angiography (DSA) and three-dimensional radiographic angiography (3DRA) were performed with bi-plane angiography equipment (Philips V5000) for pre-embolization assessment of the aneurysm. The 3DRA was performed with a C-arm rotation of 180°. The embolization procedure was then performed by an interventional neuroradiologist, together with a neurosurgeon, with the aim of total occlusion of the aneurysm. Only Guglielmi detachable coils and matrix coils (Target Therapeutics, Boston Scientific Corporation, Fremont, Calif.) were used in this study. A 3DRA procedure was performed immediately after completion of the embolization procedure, which was routine in the authors' institution, for the assessment of the immediate angiographic outcome of coil embolization. Local ethics committee approval for post-coiling 3DRA was not considered necessary for this group of patients because post-coiling 3DRA was routine practice in the institution.

The reconstructed three-dimensional model of the aneurysm and its adjacent arteries from the 3DRA was studied by two neuroradiologists separately. The long axis of the aneurysm, the longest and shortest diameters of the body of the aneurysm in the transverse plane with the greatest dimensions, and the longest diameter of the neck of the aneurysm were measured (Fig. 1). The ratio of the length of the long axis to the average transverse diameter was calculated. The angle of the long axis (α) was measured to indicate the degree of angulation of the body of aneurysms with an angulated configuration (Fig. 2). When there was a discrepancy in the measured value between the two neuroradiologists, the average value was taken. The presence of a daughter sac or lobulation was identified and its size was noted.

The quantity of each specific type of embolization coil used for embolization of each aneurysm was recorded. The actual volume of solid coils in the coil mass of each aneurysm in cubic millimeters was calculated from the sum of the volume of each individual coil. The volume of each individual coil was calculated from the product of $\pi r^2 l$, where r is the radius of each specific type of coil in millimeters as provided by the manufacturer, and l is the length of the coil in millimeters. The volume of the embolization coil mass (M) as delineated by the outer surface of the coil mass was calculated from the volumetric datasets obtained on 3DRA. Based on these results, the proportion by volume of solid coil within the coil mass (M) was calculated for each aneurysm.

Postcoiling distension of an aneurysm was diagnosed if the volume after coiling was greater than that before coiling. The degree of distension of an aneurysm was taken as the percentage increase in volume. The volume of a precoiling aneurysm (V) was defined as the volume of that part of the aneurysm that was subsequently coiled, excluding those parts of the precoiling aneurysm and small localulations that were not subsequently occupied by coils. The volume of a postcoiling aneurysm was defined as the volume of that part of the aneurysm occupied by the coil mass (M), which was equivalent to the volume of the coil mass (volume M). The distensibility of an aneurysm was taken as the greatest degree of distension that had not resulted in rupture.

Fig. 1 Dimensions of an aneurysm: L long axis, T_{ma} longest diameter of the body in the transverse plane with the greatest dimensions, T_{mi} shortest diameter of the body in the transverse plane with the greatest dimensions, N longest diameter of the neck



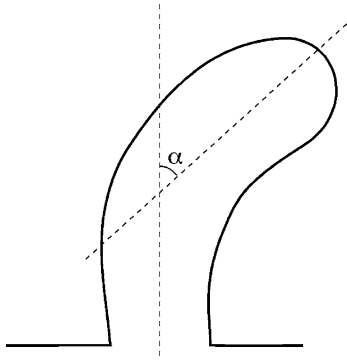


Fig. 2 Angulation of the long axis of an aneurysm. α is the angle of angulation

Volumes M and V were calculated from volumetric datasets of 3DRA performed immediately before and after coiling. The calculation of M and V consisted of two steps: first, image matching between the pre- and postcoiling datasets, and second, extraction of V from the precoiling dataset and M from the postcoiling dataset.

In the first step, the postcoiling dataset was resampled with the same spatial resolution as in the precoiling dataset. Noise in the two datasets was reduced using an anisotropic diffusion based filter, which was based on the gradient magnitude-based diffusion equation of Perona and Malik [9]. The resampling and noise reduction operations were performed for the sake of the subsequent registration algorithm that matched the two datasets on a single reference coordinate frame. A multiresolution and mutual information-based image registration framework for dataset matching was used [10, 11]. This algorithm used two 3D datasets as parameters. The precoiling dataset was taken as the fixed dataset, and the postcoiling dataset was taken as the moving dataset. The algorithm estimated iteratively the rigid transformation that aligned the moving dataset onto the fixed dataset. The algorithm terminated when the solution converged or after completing a user-defined number of iterations. The estimated rigid transformation was then applied to the moving dataset to obtain the registered (matched) dataset of the postcoiling dataset.

In the second step, after the pre- and postcoiling datasets had been registered, volume V in the precoiling dataset was extracted using a threshold-based region-growing algorithm [10]. A user gave a seed point within the vascular structure to define the region of interest. This region was allowed to grow to engulf neighboring voxels in the six-connectivity system defined in a three-dimensional space that had intensity values higher than the user-defined threshold. Volume M was extracted from the postcoiling dataset in the same fashion. The niches inside the coil volume and the small gaps on the surface of that volume were filled using the three-dimensional morphological closing operation if needed.

The volume of aneurysm distension was defined as the surplus of volume M with respect to volume V. In order to

calculate the surplus volume, volume M was partitioned into two parts, an included volume A and a protruded volume B. Volume A was the portion of volume M that was lying within volume V. Volume B was the portion of volume M that protruded from the surface of volume V. Numerically, volume A was equivalent to volume V. In some cases in which there was a displacement of the aneurysm after coiling, the coil mass was displaced relative to the position of the precoiling aneurysm; in these cases, volume A could be underestimated and volume B could be overestimated. To eliminate this error arising from aneurysm displacement, the volume of aneurysm shift, defined as the volume of the gap between the endoluminal surface of the precoiling aneurysm and the outer surface of the endoluminal coil mass, was extracted manually from volume V with reference to the shape of volume M, and labeled as volume C (Figs. 3 and 4).

The percentage increase in volume of the aneurysm as a result of coil embolization, that is the degree of postcoiling distension, was calculated from the following equation:

$$\text{Degree of distension} = \frac{\text{vol.B} - \text{vol.C}}{\text{vol.A} + \text{vol.C}} \times 100\%$$

The occurrence of beam-hardening artifacts has been noted in 3DRA although they can be reduced with an angle of rotation extended to 180° [12]. To evaluate the possible overestimation of volumes V and M due to beam hardening, five solid steel spheres of diameters 2.99, 3.97, 5.00, 5.99, and 6.99 mm, respectively, were used to simulate the pretreatment aneurysms and coil masses to study the possible effect of beam hardening on volumetric estimation with segmentation of the 3DRA volumetric dataset. The steel spheres were scanned with the same angiography

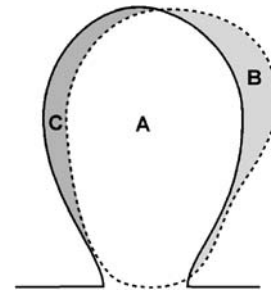


Fig. 3 Volumetric analysis. The solid line represents the boundary of the precoiling aneurysm (V). The dotted line represents the boundary of the embolization coil mass (M). Volumes A and B represent the portions of the coil mass (volume M) in relation to the precoiling aneurysm (volume V) when the 3DRA volumetric dataset of the coil mass is superimposed on that of the precoiling aneurysm. Volume A represents the portion of the coil mass that lies within the precoiling aneurysm. Volume B represents the portion of the coil mass that has protruded from the surface of the precoiling aneurysm. Volume C occurs when there is a displacement of the aneurysm after coil embolization; it represents the volume of the gap between the endoluminal surface of the precoiling aneurysm and the surface of the endoluminal coil mass

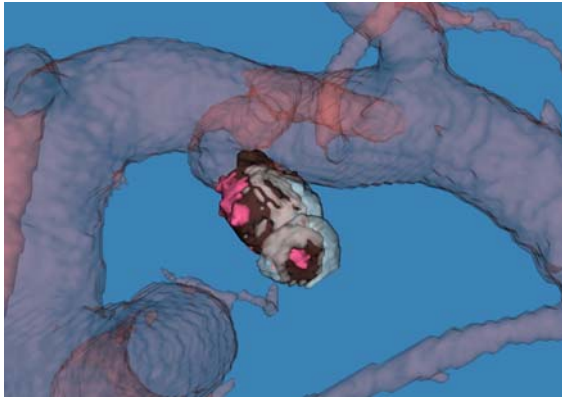


Fig. 4 Three-dimensional reconstructed image of a posterior communicating artery aneurysm with precoiling 3DRA volumetric dataset matched with the postcoiling dataset. The aneurysm was small and located at the origin of the posterior communicating artery which was preserved after coiling. The part of the aneurysm in *dark brown* represents volume A; the part in *white* represents volume B; the part in *pink* represents volume C

equipment (Philips V5000) and segmented from the 3DRA volumetric dataset with the same methodology and by the same operator as that for segmentation of vascular structures and coil masses in the tested clinical datasets,

Table 1 Characteristics of the aneurysms (L length of the long axis, T_{ma} length of the longest diameter of the body in the transverse plane with the greatest dimensions, T_{mi} length of the shortest transverse diameter of the body in the transverse plane with the

Aneurysm no.	Dimensions (mm)				Lobulation (mm×mm)		
	L	T _{ma}	T _{mi}	N	L/T ratio	α	
1	4.7	3.1	2.0	4.1	1.84	0	1.0×0.9 (coiled)
2-1	5	3.9	3.2	2.1	1.41	40	0
2-2	2.7	4	2.9	1.4	0.78	0	0
3	3.2	3.3	3.2	1.7	0.98	0	0
4	4.9	2.3	2.1	1.3	2.23	60	0
5	5.75	5.05	4.8	1.18	1.17	30	0
6	4.2	2.6	2.6	2.6	1.61	100	2.1×2.2
7	4.1	2.8	2.5	2.5	1.55	0	2.3×1.8 (coiled)
8-1	4.2	2.3	1.9	1.7	2	0	1.5×1.3
8-2	3	2	1.7	1.4	1.62	0	0
9	4.2	3.0	2.9	1.4	1.42	0	0
10	3.6	2.8	2.5	1.3	1.36	0	1.2×1.3
11	7.98	5.76	5.35	3.08	1.44	0	2.3×1.9
12	7.58	3.24	2.93	2.43	2.46	60	0
13	2.5	1.9	1.5	1.5	1.47	10	1.8×1.6 (coiled)
14	8.9	6.2	4.2	3.7	1.71	124	0
15	12	8.9	8.7	8.4	1.36	0	0
16	5.6	4.7	4	3.7	1.29	15	1.4×1.2 (coiled) 3×1.4 (coiled)
17	4.82	5.27	4.95	2.7	0.94	0	0
18	5.7	3.68	3.24	2.17	1.65	10	0
19	14	13.5	11.2	4.4	1.13	0	2.6×3.4
20	6.74	6.3	4.98	4.74	1.19	0	3.3×1.2 (coiled)

to obtain a segmented volume. The actual volumes of the solid steel spheres were calculated from their diameters which were measured with an electronic caliper. The segmented volumes of the steel spheres were then compared with the actual volumes.

Results

The characteristics of the aneurysms are shown in Table 1. CT revealed no evidence of intraluminal thrombus in the 22 aneurysms. Total occlusion was achieved in all aneurysms. There was no procedure-related rupture of an aneurysm. The findings of the volumetric analysis of the aneurysms are shown in Table 2. The percentage by volume of solid coil within the coil mass ranged from 15.78% to 82.01% in the present series. All aneurysms showed distension which ranged from 0.09% to 34.23%. The distensibility of the aneurysms was 34.23%.

The specific type, size and length of the embolization coils used in each aneurysm are shown in Table 3.

The results of the steel sphere simulation study are outlined in Table 4. Comparison between the segmented volumes and the actual volumes of the steel spheres showed that the segmented volumes of the smallest and

greatest dimensions, N length of the longest transverse diameter of the neck, L/T ratio ratio of the length of the long axis to the average transverse diameter of the body measured in the transverse plane with the greatest dimensions, α angle of angulation of the long axis)

Table 2 Volumetric analysis of the aneurysms (*M* volume of the coil mass, *A* portion of the coil mass lying within the precoiling aneurysm, *B* portion of the coil mass protruding from the surface of the precoiling aneurysm, *C* volume of the gap between the endoluminal surface of the precoiling aneurysm and the surface of the endoluminal coil mass, i.e. displacement of the aneurysm after embolization)

Aneurysm no.	Volume solid coil (mm ³)	M (mm ³)	Percentage by volume of solid coil in coil mass (%)	A (=V) (mm ³)	B (mm ³)	C (mm ³)	Degree of aneurysm distension (%)
1	6.8608	15.2396	45.02	13.6498	1.5898	0	11.65
2-1	12.6672	29.16	43.44	27.1941	1.9659	1.1364	2.92
2-2	7.917	12.6792	62.44	11.8983	0.7809	0	6.56
3	15.4342	63.1809	24.43	52.5177	10.6632	0	20.30
4	6.3336	21.4393	29.54	14.9669	6.4724	1.0045	34.23
5	21.3341	62.1407	34.33	58.7133	3.4274	0	5.84
6	9.5004	27.0749	35.09	25.9279	1.147	0.1666	3.76
7	8.4442	13.8893	60.79	12.1931	1.6962	0.7924	6.96
8-1	6.7348	19.086	35.29	17.491	1.595	0	9.12
8-2	1.8704	9.8643	18.96	8.6709	1.1934	0	13.76
9	7.7642	30.3625	25.57	24.79	5.5699	0	22.47
10	11.0838	13.5152	82.01	12.3811	1.1341	1.0936	0.30
11	75.5961	166.3403	45.45	157.5359	8.8044	0	5.59
12	18.4718	27.905	66.19	26.701	1.204	0	4.51
13	4.7502	30.0939	15.78	24.9265	5.1674	0	20.73
14	15.6856	70.7987	22.15	61.0913	9.7074	5.7892	5.86
15	152.6952	468.0515	32.62	465.0581	2.9934	2.5693	0.09
16	9.823	47.2222	20.80	46.5237	0.6985	0	1.5
17	32.986	106.4366	30.99	99.8963	6.5403	1.6466	4.82
18	20.1861	60.1314	33.700	49.3909	10.7405	0	21.75
19	286.9018	1142.978	25.10	1065.2873	77.6907	28.4111	4.51
20	45.1224	131.1264	34.41	123.1014	8.025	0	6.52

largest steel spheres were slightly underestimated by from 1.68% to 4.64%, whereas the segmented volumes of the other spheres were slightly overestimated by from 0.57% to 2.6%. The estimated diameters of the steel spheres as calculated from the respective segmented volumes were found to be of subvoxel length (voxel size 0.139446 mm).

Discussion

Theoretically there are two ways to exclude a saccular aneurysm from arterial blood flow while preserving the patency of the parent vessel. The first is endoluminal occlusion of the aneurysm, commonly with embolization coils. The second is endoluminal stent grafting of the aneurysmal vascular segment with covered stents. For intracranial aneurysms, the technique of endoluminal occlusion has been developed and evolved over the last 15 years [13–15], so much so that it has become a well-established treatment option in many centers. However, the technology cannot yet support endoluminal stent grafting of intracranial vessels.

Endoluminal packing of an aneurysm with embolization coils mechanically demands that the coil mass conform to the aneurysm sac, and counteracting this, that the aneurysm

contain the coil mass. Depending on the size and rigidity of the coil loops, a certain degree of outwardly expanding force is exerted by the coil mass against the wall of the aneurysm sac, which needs to be counteracted by the tension in the wall of the aneurysm. Based on this theory, it was hypothesized that endoluminal packing of the aneurysmal sac could be associated with a certain degree of distension of the aneurysmal sac.

When an aneurysm is filled with endoluminal embolization coils, some part of the aneurysm may not be occupied by coils, which could be due to a mismatch between the configuration of the aneurysm and that of the coil mass, irregularity in the surface of the aneurysm, or the presence of a daughter sac. With the use of the methodology described in this study, the presence of such an uncoiled part of an aneurysm could be revealed when the 3DRA volumetric dataset of the precoiling aneurysm is matched with that of the postcoiling aneurysm. Such an uncoiled part of an aneurysm would not be clearly delineated on the postcoiling 3DRA dataset if such a dataset matching technique was not employed, because these uncoiled parts would normally not be outlined with angiographic contrast after coil embolization when the aneurysm lumen was occluded by the coil mass. Since the main concern in the present study was the detection of

Table 3 Specifications of the embolization coils used. The values presented are the size of the coil loops (mm)/total length of the coil (cm)

Aneurysm no.	Matrix coils							Guglielmi detachable coils						
	3D			2D				GDC-18 standard			GDC-10			
	Firm	Standard	Soft	Firm	Standard	Soft	Ultrasoft	3D	2D	3D	2D	Standard	Soft	Ultrasoft
1			3/4				2/4							
2-1							4/8, 3/8							
2-2							3/6, 2/4							
3										5/10	4/10, 3/12			
4							3/6, 2/2							
5						5/15	3/12, 2/4							
6							3/6, 2/6							
7		3/4					2.5/6							
8-1										3/4			3/6, 2/4	
8-2													2/4	
9										4/6	3/6		2/4	
10							3/14							
11					7/30	5/45	4/8							
12		4/8					4/8, 2/6							
13							2/6							
14							3/8						4/8, 3/6, 2/6	
15	12/60			12/30		10/30, 8/30	4/8, 3/8							
16										5/10			3/6, 2/4	
17		5/10					3/24, 3/6							
18						5/15	3/6, 2/2							
19									14/30	14/30, 12/30, 9/30, 8/60, 7/30, 6/20, 5/30, 4/8				
20		6/15				5/14	4/16, 3/6							

aneurysm distension as a result of coil embolization, these uncoiled parts of an aneurysm were excluded and the volume of the coil mass was taken as the volume of the postcoiling aneurysm. For the same reason, when calculating the volume of the precoiling aneurysm, only that portion of the aneurysm that was subsequently occupied by

embolization coils was included and the uncoiled part excluded. Again, the use of the technique of volumetric dataset matching was essential for such a calculation to be feasible. Volumetric calculation was facilitated with segmentation of the volume M into volumes A and B. The error in volumetric calculation due to postcoiling shifting

Table 4 Results of steel sphere simulation study

Actual diameter of sphere (mm)	Actual volume of sphere (mm ³)	Segmented volume of sphere (mm ³)	Volumetric error (%)	Calculated diameter from segmented volume (mm)	Difference in diameter (mm)
6.99	178.8258	175.8280	-1.68 ^a	6.95	-0.04 ^a
5.99	112.5328	113.1694	0.57	6.00	0.01
5.00	65.4498	65.8555	0.62	5.01	0.01
3.97	32.7620	33.6124	2.6	4.00	0.03
2.99	13.9963	13.3463	-4.64 ^a	2.94	-0.05 ^a

^aNegative values indicates a reduction in the value when the calculated value was compared to the actual value

of the aneurysm was eliminated with the detection and calculation of volume C.

Another potential source of error was the presence of intraluminal thrombus within the aneurysm cavity, which would lead to underestimation of the volume of precoiling aneurysm in the 3DRA dataset (volume V). Embedding of embolization coils into the intraluminal thrombus would be wrongly perceived as an indication of protrusion of the coil mass beyond the margin of volume V and wrongly interpreted as indicating aneurysm distension. Specific attention was paid to detecting the presence of intraluminal thrombus in the 22 aneurysms. As CT provided no evidence of the presence of intraluminal thrombus in the 22 aneurysms, it was believed that intraluminal thrombus as a source of error in the current study could be neglected.

A third potential source of error was overestimation of the segmented volume of the 3DRA dataset due to beam-hardening artifacts. Based on the results of the steel-sphere simulation study, it is reasonable to conclude that the error of volume overestimation due to beam hardening was negligible and unlikely to have affected the findings of postcoiling aneurysm distension.

In the present study endoluminal packing of intracranial saccular aneurysms with embolization coils caused a certain degree of distension in all the aneurysms, with the degree of distension being up to 34.2%. Although postcoiling distension of the aneurysms in this study did not result in rupture, one cannot exclude the theoretical risk that endoluminal distension may lead to rupture of an aneurysm. Even though distension may not occur at the weakest point of an aneurysm, the shearing force from the distension could be transmitted to a weak point to cause a tear. On the other hand, aneurysm distensibility of up to 34.2% in this study indicates that intracranial aneurysms

can tolerate a certain degree of endoluminal distension without the risk of immediate rupture, even in aneurysms that have ruptured recently.

Nevertheless, it would be valuable to identify the potential causes of such distension and explore possible means to minimize its occurrence. One of the potential causes of aneurysm distension as identified in the present study is the selection of over-sized embolization coils. In patient 3, the length and maximum transverse diameter of the aneurysm were 3.2 mm and 3.3 mm, respectively, and the size of first coil was 5 mm, resulting in a distension of 20.3%. An over-sized first coil was selected in this patient probably because of overestimation of the aneurysm size, which could have been due to the magnification effect on DSA or selection of an inappropriately low density threshold for the reconstruction of the 3DRA images. Other factors that were considered to be potentially associated with aneurysm distension were analyzed, including a smaller size of the aneurysm, a higher ratio of the length to the average transverse diameter of the aneurysm, the first embolization coil being larger than the greatest transverse diameter of the aneurysm, a greater angle of angulation of the long axis of the aneurysm, and a higher ratio of volume of solid coil to volume of the coil mass. Each of these factors was studied to determine its relationship with the frequency of a significant degree of distension of the aneurysm by 10%. This analysis (Table 4) showed that an aneurysm of size 5 mm or less was associated with a numerically higher frequency of significant aneurysm distension than an aneurysm of size 5 mm or greater. An elongated aneurysm with a length to width ratio greater than 1.5 was associated with a numerically higher frequency of significant aneurysm distension than an aneurysm with a length to width ratio less than 1.5.

Table 5 Factors affecting degree of aneurysm distension

Factor	Proportion of aneurysms with distension $\geq 10\%$	Fisher's exact test	
		<i>P</i> value	Difference (95% CI)
Size of aneurysm (mm)			
≤ 5	6/13 (46.1%)	0.1649	35.1% (-9.1% to 74.0%)
> 5	1/9 (11.1%)		
Length to transverse diameter ratio			
> 1.5	4/9 (44.4%)	0.3762	21.3% (-21.2% to 66.5%)
< 1.5	3/13 (23.1%)		
Coil size relative to greater transverse diameter (Tma)			
Coil $< T_{ma}$	2/7 (28.6%)	1.0000	-4.7% (-53.9% to 40.5%)
Coil $> T_{ma}$	5/15 (33.3%)		
Angulation of long axis			
$> 30^\circ$	1/6 (16.7%)	0.1649	20.8% (-66.5% to 27.9%)
$< 30^\circ$	6/16 (37.5%)		
Solid coil to coil mass ratio			
$< 30\%$	5/8 (62.5%)	0.9524	48.2% (4.4% to 85.8%)
$> 30\%$	2/14 (14.3%)		

Although the sample size for this analysis was small and Fisher's exact test did not show a statistically significant difference between the two groups of comparison, these results suggest that there was probably a higher chance of aneurysms of size 5 mm or less, and aneurysms with a length to width ratio greater than 1.5 to be associated with significant distension. From the results shown in Table 5, aneurysms with a greater angle of angulation of the long axis and aneurysms with a greater coil-packing density were associated with a numerically lower frequency of significant aneurysm distension, indicating that these two factors are unlikely to be associated with aneurysm distension. The use of coils of size greater or lower than the greatest transverse diameter of the aneurysm did not seem to make a difference in the frequency of aneurysm distension.

The findings of the current study probably allow us to understand better the mechanism of resolution of the mass effect in a coiled aneurysm. It is known that most patients with aneurysm-related cranial nerve deficit recover from their symptoms after embolization of the aneurysm. The findings of the current study probably offer evidence to support the "pulsatility" theory instead of the "mass effect" theory as a cause of cranial nerve deficit in patients with

intracranial aneurysms. Given that the volume of an aneurysm, and therefore the "mass effect" of the aneurysm, may actually increase after coil embolization, recovery of cranial nerve deficit after coil embolization is unlikely to be due to resolution of the "mass effect"; rather, it is more likely to be due to resolution of the aneurysm pulsation following coil embolization.

In conclusion, endoluminal packing of intracranial saccular aneurysms with embolization coils could cause a certain degree of distension in aneurysms treated with coil embolization, with a degree of distension up to 34.2%. Intracranial aneurysms could tolerate a certain degree of endoluminal distension without a risk of immediate rupture, even for aneurysms that have ruptured recently.

Acknowledgements The authors would like to thank Mr. Clinton Wong for providing technical support in the study of embolization coils, and Miss Mi Lau for preparing the manuscript. Thanks also go to Dr. Kwok-Kuen Shing who took part in measuring the dimensions of the reconstructed three-dimensional model of the aneurysms.

Conflict of interest statement We declare that we have no conflict of interest.

References

- Rinkel GJ, Djibuti M, Algra A, Van Gijn J (1998) Prevalence and risk of rupture of intracranial aneurysms: a systematic review. *Stroke* 29:251–256
- Hop JW, Rinkel GJ, Algra A, Van Gijn J (1997) Case fatality rates and functional outcome after subarachnoid hemorrhage: a systematic review. *Stroke* 28:660–664
- Linn FH, Rinkel GJ, Algra A, Van Gijn J (1996) Incidence of subarachnoid hemorrhage: role of region, year, and rate of computed tomography: a meta-analysis. *Stroke* 27:625–629
- International Study of Unruptured Intracranial Aneurysms Investigators (2003) Unruptured intracranial aneurysms: natural history, clinical outcome, and risks of surgical and endovascular treatment. *Lancet* 362:103–110
- Juvela S, Porras M, Heiskanen O (1993) Natural history of unruptured intracranial aneurysms: a long-term follow-up study. *J Neurosurg* 79: 174–182
- Johnston SC, Higashida RT, Barrow DL et al (2002) Recommendations for the endovascular treatment of intracranial aneurysms: a statement for health-care professionals from the Committee on Cerebrovascular Imaging of the American Heart Association Council on Cardiovascular Radiology. *Stroke* 33:2536–2544
- Macdonald RL, Mojtahedi S, Johns L, Kowalczyk A (1998) A randomized comparison of Guglielmi detachable coils and cellulose acetate polymer for treatment of aneurysms in dogs. *Stroke* 29:478–485
- Stiver SI, Porter PJ, Willinsky RA, Wallace MC (1998) Acute human histopathology of an intracranial aneurysm treated using Guglielmi detachable coils: case report and review of the literature. *Neurosurgery* 43:1203–1208
- Perona P, Malik J (1990) Scale-space and edge detection using anisotropic diffusion. *IEEE Trans Pattern Anal Machine Intell* 12(7):629–639
- Kitware (2005) ITK. NLM insight: segmentation and registration toolkit. Kitware, Clifton Park, New York. <http://www.itk.org>
- Wells WM, Viola P, Atsumi H, Nakajima S, Kikinis R (1996) Multi-modal volume registration by maximization of mutual information. *Med Image Anal* 1(1): 35–51
- Hagen G, Wadstrom J, Eriksson LG, Magnusson P, Magnusson M, Magnusson A (2005) Three-dimensional rotational angiography of transplanted renal arteries: influence of an extended angle of rotation on beam-hardening artifacts. *Acta Radiol* 46(2):170–176
- Nichols DA (1993) Endovascular treatment of the acutely ruptured intracranial aneurysm. *J Neurosurg* 79:1–2
- Guglielmi G, Viouela F, Docksiler G (1995) Coil-induced thrombosis of intracranial aneurysms. In: Maciunas R (ed) *Endovascular neurological intervention*. American Association of Neurological Surgeons, pp 179–188
- Graves VB, Strother CM, Duff TA et al (1995) Early treatment of ruptured aneurysms with Guglielmi detachable coils: effect on subsequent bleeding. *Neurosurgery* 37:640–648